

# Shrinkage and Springback Behavior of Methylsilsesquioxanes Prepared by an Acid/Base Two-Step Processing Procedure

Hanjiang Dong,<sup>†</sup> Richard F. Reidy,<sup>‡</sup> and John D. Brennan<sup>\*,†</sup>

Department of Chemistry, McMaster University, 1280 Main Street West, Hamilton, Ontario L8S 4M1, Canada, and Department of Materials Science and Engineering, University of North Texas, Denton, Texas 76203

Received June 24, 2005. Revised Manuscript Received September 20, 2005

We report on the effect of water concentration on the shrinkage and springback behavior of methylsilsesquioxane (MSQ) materials prepared by an acid/base two-step procedure in ethanolic solutions. The morphologies of the MSQ gels were characterized by SEM, nitrogen sorption, and mercury porosimetry. The chemical structures of these gels were also determined by solid-state <sup>13</sup>C and <sup>29</sup>Si NMR. As expected, shrinkage decreases as the volume of macropores in the material increases. Some samples, however, display shrinkage followed by expansion (springback phenomenon) even in the absence of surface modification or solvent exchange. The springback effect is attributed to the intrinsic properties of MSQ monoliths, namely, hydrophobicity and a low concentration of reactive groups on the surface. The implications of these findings for the development of low-shrinkage materials are discussed.

## Introduction

Controlling the shrinkage of sol–gel-derived materials during drying presents a considerable challenge. In general, shrinkage is induced by the capillary forces within the drying material, which can reach values of between 19 and 36 MPa owing to the presence of micropores and mesopores, and is resisted by the bulk modulus of the gel.<sup>1</sup> Traditionally, shrinkage has been overcome by supercritical drying where, in principle, there is no capillary force.<sup>2</sup> However, this method is batch- and size-limited (and therefore expensive) and may be dangerous owing to the high pressures used in the process.

Two methods have been commonly used to prepare low-density silica without macropores under ambient pressure conditions.<sup>3,4</sup> In the first method, wet gels were exchanged with solvents with low surface tension, such as hexane, followed by surface modification of the silica with trimethylchlorosilane (TMCS).<sup>3</sup> In this process, the silica gel exhibits significant shrinkage during drying but expands back to nearly its original size, leading to a silica density as low as 0.1 cm<sup>3</sup>/g. This method has been further developed to directly silylate both hydrogels<sup>5</sup> and alcogels.<sup>6</sup> One key feature of

this method is the reduction in the number of reactive Si–OH groups as a result of capping with passive Si–(CH<sub>3</sub>)<sub>3</sub> groups, which prevents irreversible condensation during drying. The second method to minimize shrinkage is to age wet gels in solutions of precursors followed by solvent exchange. The increase in the gel modulus during aging allows the gel to resist the capillary force induced by small pores, and gel densities as low as 0.2 cm<sup>3</sup>/g can be obtained.<sup>4</sup> While the above methods minimize shrinkage, both methods require several solvent exchange steps and the introduction of either the precursor or organosilanes during processing. These processes are diffusion-limited and therefore time-consuming, which make them unsuitable for preparing large monolithic samples. These methods also consume significant amounts of organic solvents and, therefore, pose environmental problems.

Since capillary pressure decreases with increasing pore radius, a potential method to reduce shrinkage is to increase the volume of macropores in the material. This has been demonstrated in silica materials that were made macroporous by templating<sup>7</sup> or spinodal decomposition.<sup>8</sup> Templating methods include colloidal crystal and emulsion templating,<sup>7</sup> which have potential applications in the development of photonic crystals, chemical sensors, catalysts, and membranes. Spinodal decomposition, in most cases, relies on phase separation of an organic polymer, such as poly(ethylenoxide) (PEO), prior to gelation of silica, resulting in an interconnected macroporous material.<sup>8</sup> Such materials have been used to form monolithic columns, which are commercially available from Merck,<sup>9</sup> and show no radial

\* To whom correspondence should be addressed. Tel: (905) 525-9140 (ext. 27033). Fax: (905) 527-9950. E-mail: brennanj@mcmaster.ca. Internet: <http://www.chemistry.mcmaster.ca/faculty/brennan>.

<sup>†</sup> McMaster University.

<sup>‡</sup> University of North Texas.

- (1) Smith, D. M.; Stein, D.; Anderson, J. M.; Ackerman, W. J. *Non-Cryst. Solids* **1995**, 186, 104.
- (2) (a) Kistler, S. S. *Nature* **1931**, 127, 741. (b) Tewari, P. H.; Hunt, A. J.; Lofftus, K. D. *Mater. Lett.* **1985**, 3, 363.
- (3) (a) Smith, D. M.; Deshpande, R.; Brinker, C. J. *Mater. Res. Soc. Symp. Proc.* **1992**, 271, 567. (b) Prakash, S. S.; Brinker, C. J.; Hurd, A. J.; Rao, S. M. *Nature* **1995**, 374, 439.
- (4) (a) Hæreid, S.; Dahle, M.; Lima, S.; Einarsrud, M.-A. *J. Non-Cryst. Solids* **1995**, 186, 96. (b) Einarsrud, M.-A. *J. Non-Cryst. Solids* **1998**, 225, 1.
- (5) Schwertfeger, F.; Frank, D.; Schmidt, M. *J. Non-Cryst. Solids* **1998**, 225, 24.

(6) Land, V. D.; Harris, T. M.; Teeters, D. C. *J. Non-Cryst. Solids* **2002**, 283, 11.

(7) (a) Velez, O. D.; Lenhoff, A. M. *Curr. Opin. Colloid Interface Sci.* **2000**, 5, 56. (b) Imhof, A.; Pine, D. J. *Adv. Mater.* **1998**, 10, 697.

(8) Nakanishi, K. *J. Porous Mater.* **1997**, 4, 67.

(9) Cabrera, K. J. *Sep. Sci.* **2004**, 27, 843.

shrinkage when placed in capillaries up to 200  $\mu\text{m}$  in diameter.<sup>10</sup>

Recently, Nakanishi et al. demonstrated that the trifunctional precursor methyltrimethoxysilane (MTMS), when processed under highly acidic conditions (molar ratio MTMS: MeOH:1 M  $\text{HNO}_3 = 1:1:2$ ), could form macroporous methylsilsequioxane (MSQ) gels that showed minimal shrinkage,<sup>11</sup> even in capillaries up to 500  $\mu\text{m}$  in diameter. They attributed the low shrinkage to steric hindrance by the methyl group. More recently, our group showed that polymerization of MTMS using an acid/base two-step procedure (denoted as B2) considerably increased the range of conditions available for the formation of MSQ monolithic gels as compared to one-step methods employing only an acidic or basic catalyst.<sup>12</sup> The resulting gels exhibited various morphologies, including macroporous monoliths, without the need for templates or phase separation initiators such as PEO, which are required to create macroporous silica.<sup>8</sup>

While our initial study demonstrated the formation of macroporous MSQ materials by the B2 method, factors affecting the shrinkage of such material were not examined. In subsequent work on this system, it was determined that the water:MTMS ratio played an important role in controlling the shrinkage of MSQ materials. In this paper, we systematically investigate the effect of water concentration on MSQ morphologies and relate this to the shrinkage of the MSQ gels. Unexpectedly, we find that, under certain conditions that yield materials with an intermediate volume of macropores, the springback phenomenon is observed with no need for solvent exchange or surface modification steps. The chemical and physical properties of MSQ that influence this behavior are described.

## Experimental Section

**Chemicals.** Reagent grade methyltrimethoxysilane, tetramethylsilane (TMS), ammonium hydroxide ( $\text{NH}_4\text{OH}$ ), hydrochloric acid (HCl), and absolute ethanol (EtOH) were purchased from Aldrich (Ontario, Canada). All reagents were used as received. All water was obtained from a Milli-Q Synthesis A10 water purification system.

**Procedures.** *Formation of MSQ Gels.* Detailed procedures to prepare MSQ gels have been described in our previous report.<sup>12</sup> Briefly, 1 mL of MTMS, 0.813 mL of EtOH, and 0.02 M HCl (varying volume) were first mixed to generate hydrolyzed monomer and condensed oligomers. After 1 h of reaction, 1 M  $\text{NH}_4\text{OH}$  was added to promote rapid condensation and gelation. The volume ratio of the catalysts, 0.02 M HCl and 1 M  $\text{NH}_4\text{OH}$ , was fixed to be 1. We use  $r$  to represent the mole ratio of MTMS to water (the sum of 0.02 M HCl and 1 M  $\text{NH}_4\text{OH}$ ) and examine  $r$  values over the range from 3 to 12. As examples, samples with  $r$  values of 4, 8, and 12 corresponded to volumes of 0.02 M HCl (which is equal to the volume of 1 M  $\text{NH}_4\text{OH}$ ) of 0.25, 0.50, and 0.75 mL, respectively. The resulting gels were denoted as MSQr4, MSQr8, and MSQr12, respectively. Normally, drying was performed in air at room temperature and approximately 35% relative humidity for

at least 7 days prior to characterization of the gels. To record kinetic data on the shrinkage and springback of MSQr8, a sample was prepared in a small vial ( $14.5 \times 45$  mm) and following gelation the vial was carefully broken and the sample was placed into a larger vial ( $27.5 \times 57.5$  mm). This drying method ensures more uniform shrinkage than would be obtained by simply removing the cap from the small vial. In the latter method, we found that MSQr8 shrinks more rapidly and springs back faster on the bottom than on the top of the gel. In addition, it is very difficult to measure the sample size within the small vial. Both the linear shrinkage and the change in mass were monitored as a function of time until a constant mass was reached.

*Characterization of MSQ Gels.* Porosity measurements were performed by nitrogen sorption porosimetry (equilibrium time of 1 min) using a Quantachrome Nova 2000 and mercury porosimetry using a Quantachrome PoreMaster GT. All samples were degassed at 200  $^\circ\text{C}$  for 10 h before measurement. For nitrogen sorption studies, pore size distributions were calculated from the desorption isotherm using the BJH (Barrett, Joyner, and Halenda) model.<sup>13</sup> The total pore volume was estimated at a pressure close to  $p/p_0 = 1$ . Mercury porosimetry studies were conducted over a pressure range of 20–60000 psi using a pressure increase of 5 psi per second. Pore size distributions as a function of pore diameter were derived from the intrusion curve using the Washburn equation.<sup>14</sup> The mercury surface tension and the contact angle used in calculation were 480 dyn/cm and  $140^\circ$  (standard values for mercury porosimetry), respectively, and the pores were assumed to be cylindrical in shape. We realized that our choice of cylindrical geometry might not represent the actual pore shape in our materials, which could in fact be more slitlike based on our BET isotherms (not shown), which were of the H3 type.<sup>15</sup> However, the use of cylindrical pores provides the simplest mathematical model for calculation of pore sizes, and the error introduced by this model is expected to be small when used to measure the porosity of solids containing interconnected channels (as are observed in MSQ materials), provided that all pores are equally accessible to the exterior mercury reservoir.<sup>16</sup>

Solid-state  $^{13}\text{C}$  and  $^{29}\text{Si}$  cross polarization (CP)/magic angle spinning (MAS) NMR spectra were recorded on a Varian VXR300 spectrometer at 75 and 59.5 MHz, respectively. A total of 1000 scans were accumulated at a spinning rate of 2 kHz. Pulse width, contact time, and delay time for  $^{13}\text{C}$  were 8.5  $\mu\text{s}$ , 1 ms, and 3 s, respectively, while the corresponding values for  $^{29}\text{Si}$  were 8.5  $\mu\text{s}$ , 2 ms, and 10 s, respectively. Tetramethylsilane was used in both cases as an external reference. Images of gels were obtained using a Philips 515 scanning electron microscope (SEM) at an operating voltage of 10 kV. The surfaces were previously sputter-coated with gold to avoid charging effects during observation.

## Results and Discussion

**Shrinkage and Springback.** The linear shrinkage of MSQ gels after aging for 1 week was found to be highly dependent on the  $r$  value, as shown in the images in Figure 1. Samples that had a low  $r$  value ( $r < 5$ ) were generally translucent and typically showed significant shrinkage, with linear shrinkage values of 40–55%. Samples prepared with intermediate  $r$  values ( $r = 6$ –8) showed shrinkage initially followed by expansion (springback). Samples were translucent during shrinkage, but became opaque after springback.

- (10) Motokawa, M.; Kobayashi, K.; Ishizuka, N.; Minakuchi, H.; Nakanishi, K.; Jinnai, H.; Hosoya, K.; Ikegami, T.; Tanaka, N. *J. Chromatogr. A* **2002**, 961, 53.  
(11) Kanamori, K.; Yonezawa, H.; Nakanishi, K.; Hirao, K.; Jinnai, H. *J. Sep. Sci.* **2004**, 27, 874.  
(12) Dong, H.; Brook, M. A.; Brennan, J. D. *Chem. Mater.* **2005**, 17, 2807.

- (13) Barrett, E. P.; Joyner, L.; Halenda, P. P. *J. Am. Chem. Soc.* **1951**, 73, 373.  
(14) Washburn, E. W. *Phys. Rev.* **1921**, 17, 273.  
(15) Kruk, M.; Jaroniec, M. *Chem. Mater.* **2001**, 13, 3169.  
(16) León y León, C. A. *Adv. Colloid Interface Sci.* **1998**, 76–77, 341.

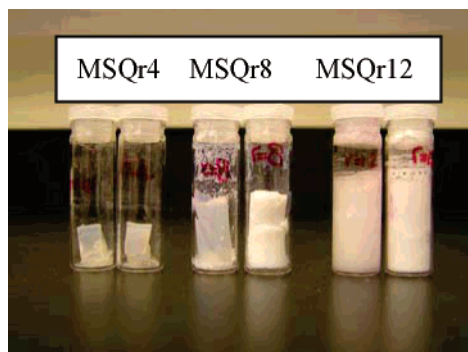


**Figure 1.** Images of MSQr4, MSQr8, and MSQr12 gels during drying and after drying; for each pair, the left sample is during drying, while the right sample is after drying.

These samples typically shrank by up to 30% initially, but then ended up with only 10% shrinkage after springback. Samples with higher  $r$  values ( $r > 9$ ) were opaque, showed only minor shrinkage ( $<10\%$ ), and did not undergo the springback phenomenon. The different appearance of MSQr8 gel during and after drying results from changes in the solvent concentration and pore morphology. During drying, shrinkage leads to a smaller pore size and perhaps a more uniform pore size distribution. The refractive index discrepancy between the solvent and the MSQ skeleton is also much smaller than that between air and the MSQ skeleton. Both of these factors cause a reduction in light scattering of the wet MSQ, and therefore this material is more transparent than the dried MSQ.

It was also observed that springback of MSQr8 materials was often accompanied by cracking. This likely resulted from a capillary force gradient in the material due to the broad pore size distribution (see below). On the other hand, MSQr12 materials, while mechanically fragile, likely had lower capillary stresses because of the high volume of macropores (see Figure 5) and thus did not crack. We are currently investigating methods to reduce the pore size distribution and the volume of small mesopores ( $<4$  nm) in an effort to avoid cracking (MSQr8) and will report on these findings in a future manuscript.

**Gelation and Phase Separation.** The shrinkage of sol-gel-derived materials depends on the degree of macroporosity and the overall connectivity and the strength of filaments connecting particles within the material. Macroporosity depends on the relative rates of gelation and phase separation;<sup>12</sup> thus, the gelation and phase separation times ( $t_g$  and  $t_{ps}$ ) for MSQr4, MSQr8, and MSQr12 were examined to better understand the origins of the shrinkage and springback behavior. As shown in Figure 2, the gelation times of MSQ gels are 150 (MSQr4), 37 (MSQr8), and 13 (MSQr12) min, respectively. The phase separation times for MSQr8 and MSQr12 were 45 and 10 min, respectively. The phase separation time for MSQr4 could not be determined accurately since it took 2 days for the transparent gel to become translucent. Thus, in MSQr4 samples  $t_g \ll t_{ps}$  and in MSQr8  $t_g$  is slightly shorter than  $t_{ps}$  ( $t_g - t_{ps} = -8$  min) while in MSQr12  $t_g$  is longer than  $t_{ps}$  ( $t_g - t_{ps} = 3$  min).

The driving force for both gelation and phase separation in MSQ gels is governed by condensation reactions.<sup>11</sup> In the range of  $r$  values we studied, the rate of condensation

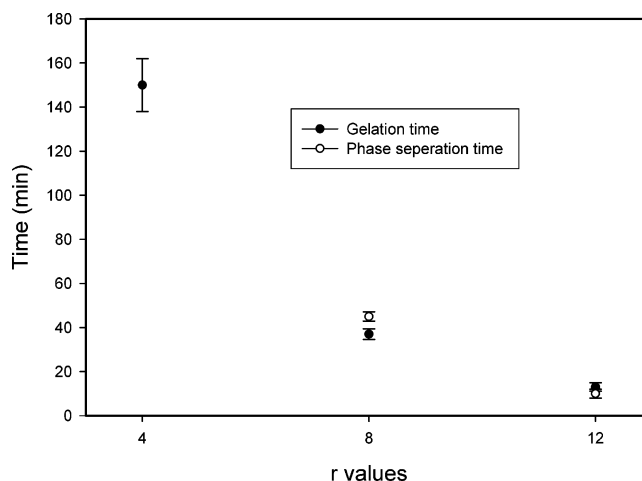


**Figure 2.** Gelation and phase separation times for MSQ samples.

increases with increasing water concentration. This explains why both  $t_g$  and  $t_{ps}$  become shorter on going from MSQr4 to MSQr12. Phase separation in MTMS systems takes place without polymer additives, which are usually required in TMOS or TEOS systems.<sup>8</sup> This is mainly due to the hydrophobicity of the intrinsic Si-CH<sub>3</sub> groups. With increasing condensation, the hydrophobic and polymerized MSQ species become immiscible with the highly polar solvents, leading to phase separation. As water concentration increases, the solvent becomes more polar and has a stronger tendency to form hydrogen bonds relative to alcoholic solvents. As a result, phase separation times decrease more rapidly than gelation times as water concentration increases, leading to a crossover between  $t_g$  and  $t_{ps}$  such that phase separation occurs prior to gelation in MSQr12.

**SEM Images.** The differences in  $t_g - t_{ps}$  as a function of water concentration significantly affect the morphologies of the resulting MSQ gels. Figure 3 shows the SEM images of the three MSQ monoliths. Two distinct differences in morphology can be observed from these images. The first difference is that the feature sizes for pores and particles increase drastically on going from MSQr4 to MSQr12, even though the magnification of MSQr12 is only one-fourth that of the other samples. (Note: we could not obtain a high-magnification image of the MSQr12 sample owing to charging effects.) Macropores are clearly present in MSQr8 ( $t_g - t_{ps} = -8$  min) and MSQr12 ( $t_g - t_{ps} = 3$  min), while no macropores could be observed in MSQr4 ( $t_g \ll t_{ps}$ ). This result highlights the importance of the relative times of gelation and phase separation as one of the major factors controlling the morphologies of sol-gel-derived MSQ materials. Only when  $t_g$  and  $t_{ps}$  are comparable can monoliths with macropores be generated, and the pore sizes increase with the increase in the value of  $t_g - t_{ps}$ .

The second difference in morphology observed in the SEM images relates to the nature of the pore networks. MSQr8 and perhaps also MSQr4 have an interconnected pore and particle network. In contrast, MSQr12 exhibits large and distinct aggregates assembled from either ellipsoidal or spherical particles on the order of 1–5  $\mu\text{m}$  in diameter. The reason for this remains unclear. It may relate to the rapid gelation and highly polar solvents used to form MSQr12.



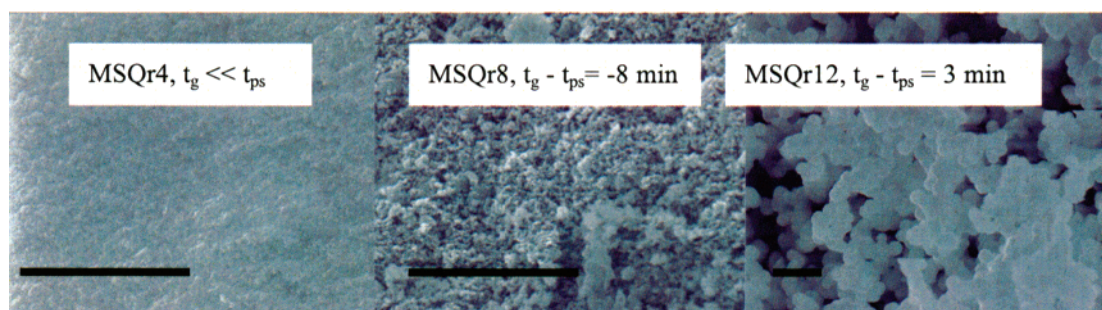


Figure 3. SEM images of MSQ gels: MSQr4, MSQr8, and MSQr12, bar = 5  $\mu\text{m}$ .

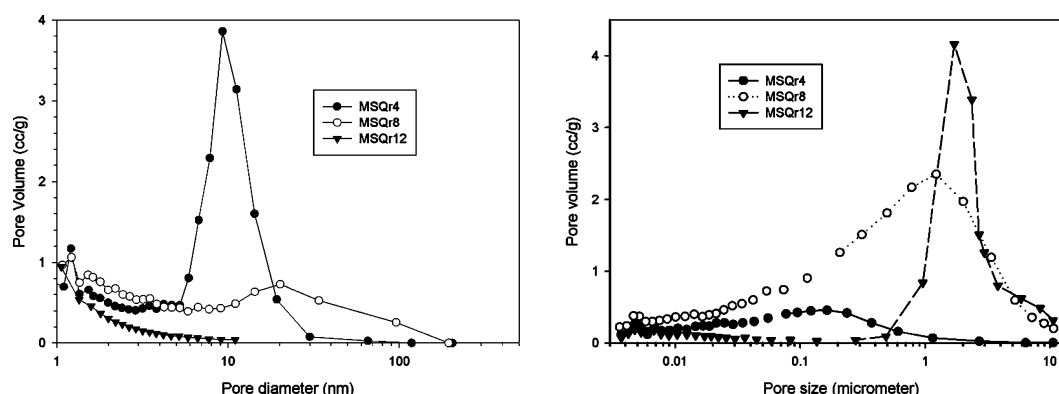


Figure 4. Pore size distributions of MSQ gels (left panel, nitrogen sorption; right panel, mercury porosimetry).

This material had very poor mechanical properties because of both its low density ( $0.205 \text{ g/cm}^3$ ) and the aggregated nature of the particles in the gel, resulting in poor connectivity.

**Morphology of MSQ Gels.** To obtain a clearer picture of the relationship between morphology and shrinkage, we performed nitrogen sorption and mercury porosimetry measurements to obtain quantitative data on porosity. Figure 4 shows the pore size distributions of MSQ gels. Nitrogen sorption (left panel) results clearly demonstrate significant differences in the pore size distributions for the three samples. The major changes in pore size distributions occurred for mesopores with pore diameters larger than 2 nm. MSQr4 materials showed a relatively narrow mesopore size distribution with a median diameter of 8 nm, while MSQr8 materials showed a much broader mesopore size distribution centered at 20 nm. On the other hand, MSQr12 materials had no mesopores larger than  $\sim 12 \text{ nm}$ .

Similar to nitrogen sorption analysis, mercury porosimetry data (Figure 4, right panel) show that these materials have broad pore size distributions. The relatively sharp curve for MSQr12 correlates well with the cluster separation observed by SEM, but it must be noted that the sample cracked during measurement, which could have led to some alteration in the macropore diameters measured.<sup>17</sup> Compression of materials has been reported during mercury porosimetry of silica gels,<sup>17</sup> which could lead to cracking. Although the MSQr8 material has a significant volume of macropores, no cracks were observed in this material after measurement, suggesting that the porosimetry data reflects the true macropore distribu-

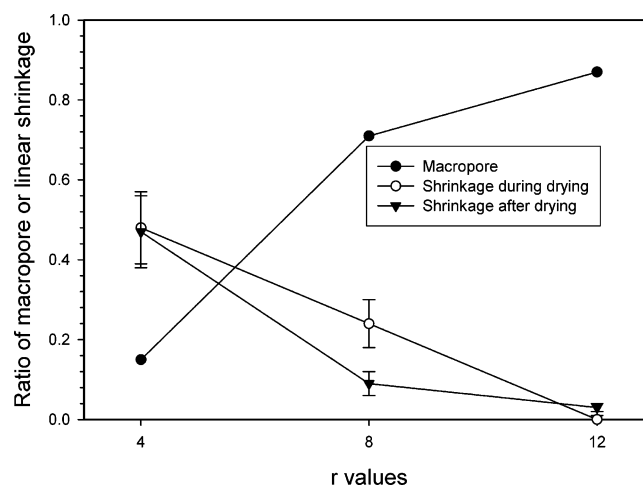
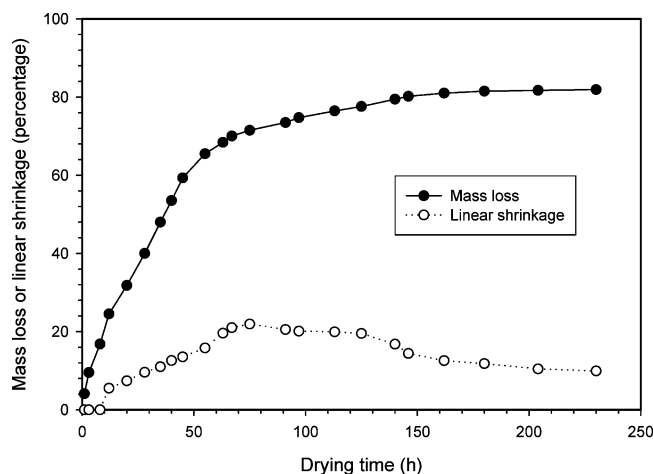


Figure 5. Relationship between ratio of macropores and linear shrinkage of MSQ gels during and after drying.

tion in the material. Nevertheless, it is possible that compression could lead to an underestimation of the pore volumes of macropores, as discussed below.

Figure 5 displays the relationship between the  $r$  value and the ratio of macropore volume ( $> 50 \text{ nm}$  diameter) to the total pore volume and the maximum linear shrinkage during drying and after drying of the three MSQ samples. Pore sizes bigger and smaller than 50 nm are obtained by mercury porosimetry and nitrogen sorption, respectively. As shown in Figure 5, the ratio of macropore volume increases from 15% (MSQr4) to 71% (MSQr8) to 87% (MSQr12). Considering the fact that the macropore volume is likely underestimated in MSQr12 and to a lesser degree MSQr8, the latter two numbers could be even higher. As a result, the capillary force exerted on MSQr4 and MSQr12 during drying are highest and lowest, respectively. Although the

(17) (a) Pirard, R.; Blacher, F.; Pirard, J. P. *J. Mater. Res.* **1995**, *10*, 2114.  
(b) Scherer, G. W.; Smith, D. M.; Qiu, X.; Anderson, J. J. *Non-Cryst. Solids* **1995**, *186*, 316.



**Figure 6.** Mass loss and linear shrinkage of MSQr8 as a function of drying time.

bulk modulus increases with the decrease in the  $r$  value due to the increased density and the higher particle connectivity, the induced capillary force apparently overcomes the resistance of the higher bulk modulus in MSQr4, leading to its significant shrinkage during drying (up to 50%). The ratio of macropore volume in MSQr8 lies between the other two gels and the size of most mesopores in this sample are much bigger than those in MSQr4. Consequently, MSQr8 has less shrinkage compared to MSQr4 and most of the contracted body recovers after drying.

Figure 6 shows a detailed evolution of both the linear shrinkage and mass change during drying of the MSQr8 material. Assuming that the condensation reactions are complete, the composition of MSQr8 before drying is 19.6% MeOH, 24.6% EtOH, 38.6% H<sub>2</sub>O, and 17.2% MSQ by weight. The final mass loss, as shown in Figure 6, is 81.9%, which is close to the value of 82.8% that would be obtained upon complete loss of solvent. The small difference may be due to residual unhydrolyzed or uncondensed groups Si–OX (X = H, CH<sub>3</sub>, C<sub>2</sub>H<sub>5</sub>, and see Figure 7), which will increase the mass of MSQ compared to the case where complete condensation occurs. The change of mass can be roughly divided into two periods, corresponding to rapid loss of mass over the first 55 h (65%) followed by a much slower loss of mass over the remaining 175 h (17%). This reflects the rapid loss of the more volatile alcohol followed by the slower loss of water. The 65% mass loss is much higher than the combined value of MeOH and EtOH weight (44.2%), indicating that there is also some loss of water during the initial stages of drying.

The shrinkage of the material generally increases during the period where the rapid mass loss occurs. However, shortly after the slower period of mass loss begins, the dimensions of the gel begin to stabilize and become relatively constant during the period from 70 to 120 h. Beyond 120 h the material undergoes a relatively rapid expansion until  $t = 160$  h, followed by a very slow expansion until 230 h. The rapid period of springback corresponds to the point where most of the entrapped water is evaporated, suggesting that springback occurs at a nearly dry state.

The changes in the mass of the gels are different for different materials (data not shown) and do not correlate to

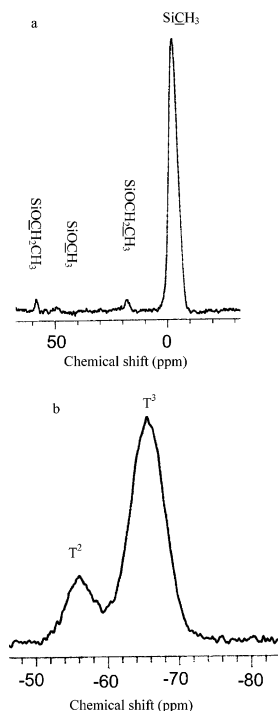


**Figure 7.** CP/MAS <sup>13</sup>C (a) and <sup>29</sup>Si (b) NMR spectra of MSQr8 with assignments.

volume changes. One would expect a higher rate of mass loss with a high  $r$  value because these materials have more and larger macropores. However, the rate of mass loss is MSQr4 > MSQr8 > MSQr12. There are basically two factors that affect the rate of mass loss under identical conditions (e.g., temperature, pressure, and humidity): the composition of the volatile solvents and the pore morphology (e.g., size, shape, distribution, and connectivity). Our result indicates that the composition of the solvent plays a leading role in determining the mass loss. The relatively high concentration of methanol in MSQr4 leads to fast weight loss for this gel compared to the other gels. The volume change, on the other hand, is mainly dependent on the pore morphology. MSQr4 always displays the highest volume shrinkage of the three gels because of its small pore size.

**Chemical Properties of MSQ Gels.** To better understand the origins of the springback phenomena, we also examined the chemical properties of the MSQr8 material using solid-state NMR. Sol–gel materials can be regarded as an assembly of fractal clusters.<sup>18</sup> Capillary stress during drying induces cluster penetration. If the penetrated boundaries among these clusters are chemically active (e.g., owing to a large number of Si–OH groups), polycondensation may take place.<sup>18</sup> In silica gels, reducing the number of reactive groups on the surface is fulfilled by surface modification using TMCS, which offers geometric restriction of irreversible condensation during drying.<sup>3</sup> In this treatment, the hydrophilic silica surface is also made hydrophobic due to the Si–(CH<sub>3</sub>)<sub>3</sub> groups of TMCS. These two factors increase the elastic deformation in silica gels, leading to springback after the critical point of drying.<sup>1</sup>

(18) Duffours, L.; Woignier, T.; Phalippou, J. *J. Non-Cryst. Solids* **1996**, *194*, 283.

From solid-state  $^{29}\text{Si}$  NMR spectra, we have determined that the degree of condensation (DC) of these MSQ gels varies from 0.92 to 0.95, which is higher than the value of  $\sim 0.85$  found in dried silica.<sup>19</sup>  $^{13}\text{C}$  and  $^{29}\text{Si}$  CP/MAS NMR spectra of the MSQr8 are shown in Figure 7. The  $^{13}\text{C}$  spectrum clearly exhibits peaks corresponding to alkoxy groups at 58.5 ppm ( $\text{OCH}_2\text{CH}_3$ ), 18.6 ppm ( $\text{OCH}_2\text{CH}_3$ ), and 50 ppm ( $\text{OCH}_3$ ).<sup>20</sup> However, the concentrations of these residual groups are very low ( $<1.0\%$ ), indicating nearly complete hydrolysis. The  $\text{Si}-\text{OC}_2\text{H}_5$  groups originate from esterification and solvent exchange during the first acidic step because hydrolysis is reversible in the presence of acid. The largest peak at  $-3$  ppm belongs to the carbon of  $\text{Si}-\text{CH}_3$ . The corresponding  $^{29}\text{Si}$  CP/MAS NMR spectrum exhibits two Si peaks at  $-57.5$  and  $-65.5$  ppm relative to tetramethylsilane. They are ascribed to  $\text{T}^2$  ( $\text{CH}_3\text{SiO}_{2/2}(\text{OH})$ ) and  $\text{T}^3$  ( $\text{CH}_3\text{SiO}_{3/2}$ ), respectively.<sup>21</sup> The degree of condensation (DC) is defined as  $\text{DC} = \sum_n n\text{T}^n/f$ , with  $f$  being the functionality of a precursor (for MTMS,  $f = 3$ ). The relative intensity of  $\text{T}^2$  and  $\text{T}^3$  is 0.21 and 0.79; therefore, the DC is 0.93. We note here that similar values were obtained using single-pulse NMR experiments, indicating that differences in cross-polarization efficiencies for the  $\text{T}^2$  and  $\text{T}^3$  species did not distort the DC value. However, the single-pulse spectra were still very noisy, even after 1 day of data collection; thus, only the CP spectra are shown. Taking the DC value 0.93 for MSQr8 and a typical value 0.85 for silica, the empirical formulas are  $(\text{CH}_3\text{Si}(\text{OR})_{0.19}\text{O}_{1.405})_n$  (MSQ) and  $(\text{Si}(\text{OR})_{0.8}\text{O}_{1.6})_n$  (silica), where R is H,  $\text{CH}_3$ , or  $\text{C}_2\text{H}_5$  (in the case of MSQr8, R is essentially all H). This means that the number of potential reactive groups per silica in MSQ is 4 times lower than that in silica. Therefore, the two requirements for springback (hydrophobic surface due to  $\text{Si}-\text{CH}_3$  groups and low concentration of  $\text{Si}-\text{OH}$  groups) in MSQ materials are fulfilled. If shrinkage during drying is such that

the material can undergo elastic deformation, most of the contracted body will recover, as shown in MSQr8. Otherwise, significant plastic deformation due to broken and distorted  $\text{Si}-\text{O}-\text{Si}$  bonds would lead to irreversible shrinkage as in the case of MSQr4.

Finally, we should point out that, after springback, the size and shape of MSQr8 do not alter in response to external physical stimuli such as solvent and temperature. This is different from a series of papers by Rao and Dave, who studied a hybrid gel prepared by polymerization of bis[3-(trimethoxysilyl)propyl]ethylenediamine.<sup>22</sup> This hybrid gel exhibited reversible thermoresponsive changes in volume due to the co-presence of both hydrophobic and hydrophilic groups. MSQr8, on the other hand, only has hydrophobic  $\text{Si}-\text{CH}_3$  groups and has a highly cross-linked gel network after drying. Thus, this material will not respond to changes in temperature or solvent conditions.

## Conclusions

We present the effect of water concentration on the shrinkage of MSQ gels prepared by an acid/base two-step procedure. The extent of shrinkage decreases with increasing water concentration due to an increase in macropore volume. Samples prepared with an  $r$  value of 8 (MSQr8) showed springback without solvent exchange or surface modification, due to the intrinsic hydrophobicity and low concentration of reactive groups in such materials. This phenomenon may prove to be useful in the development of monolithic chromatography columns or other devices where minimal shrinkage of the material is required.

**Acknowledgment.** The authors thank the Natural Sciences and Engineering Research Council of Canada, MDS-Sciex, the Canadian Foundation for Innovation, and the Ontario Innovation Trust for financial support of this work. J.D.B. holds the Canada Research Chair in Bioanalytical Chemistry.

CM051369W

- (19) (a) Peeters, M. P. J.; Wakelkamp, W. J. J.; Kentgens, A. P. M. *J. Non-Cryst. Solids* **1995**, *189*, 77. (b) Glaser, C. A.; Wolkes, G. L.; Bronniman, C. E. *J. Non-Cryst. Solids* **1989**, *113*, 73.  
 (20) Yang, J. J.; El-Nahhal, I. M.; Maciel, G. E. *J. Non-Cryst. Solids* **1996**, *204*, 105.  
 (21) (a) Maciel, G. E.; Sullivan, M. J.; Sindorf, D. W. *Macromolecules* **1981**, *14*, 1607. (b) Engelhardt, G.; Jancke, H.; Lippmaa, E.; Samoson, A. *J. Organomet. Chem.* **1981**, *210*, 295.

- (22) (a) Rao, M. S.; Dave, B. C. *Adv. Mater.* **2001**, *13*, 274. (b) Rao, M. S.; Dave, B. C. *Adv. Mater.* **2002**, *14*, 443. (c) Rao, M. S.; Dave, B. C. *J. Am. Chem. Soc.* **2003**, *125*, 11826.